

Investigation of Mediterranean biomass pyrolysis by thermogravimetric analysis: Thermal behaviour and sensitivity of kinetic parameters

Nourelhouda Boukaous^(1,2), Lokmane Abdelouahed⁽¹⁾, Mustapha Chikhi⁽²⁾, Chetna Mohabeer⁽¹⁾, Abdeslam Hassen Meniai^{(2) *}, Bechara Taouk⁽¹⁾

1: Normandie Univ, INSA Rouen Normandie, UNIROUEN, Laboratoire de Sécurité des Procédés

Chimiques LSPC-EA 4704, 76000 Rouen, France

2: Faculté de génie des procédés, Université Salah Boubnider Constantine 3, Constantine, Algérie

* meniai@yahoo.fr

Supplementary Materials

This part shows the different tables and graphs that are related to the different results discussed in the text.

Proximate analysis protocol:

Details of the method can be found in reference 26. The method can be summarized as follows:

$$FC\% = 100 - \%Ash - VM\%$$

TG of pyrolysis of biomass sample gives the humidity and VM percent

TG of char combustion (by using air) gives the Ash percent

The author of the article recommends the use of 10 and 20 mg of biomass sample, and 40 ml/min flow for both nitrogen and air.

Mineral analysis:

The detailed mineral analysis of different biomasses can be shown in Table S.1.

Table S.1 ICP AES analysis for the five biomasses.

| | Mass (mg/kg of raw material) | | | | |
|----|------------------------------|-----------|-----------|-----------|-----------|
| | CM | OK | APH | WS | DK |
| Ag | 0.85 | 0.07 | 1.87 | 0.20 | 0.52 |
| Al | 467.17 | 107.34 | 8.75 | 268.23 | 33.46 |
| Ba | 49.11 | 0.93 | 0.27 | 26.31 | 0.56 |
| Be | < 0.00003 | < 0.00003 | < 0.00003 | < 0.00003 | < 0.00003 |
| Bi | 17.96 | 18.81 | 20.96 | 20.41 | 14.26 |
| Ca | 5735.66 | 522.90 | 1299.19 | 4067.55 | 287.49 |
| Cd | 0.50 | 0.07 | < 0.00002 | 0.02 | < 0.00002 |
| Co | < 0.0004 | < 0.0003 | < 0.0004 | < 0.0004 | < 0.0003 |
| Cr | 2.39 | 1.38 | 2.17 | 4.55 | 1.34 |
| Cu | 4.63 | 3.01 | 6.34 | 5.95 | 4.98 |
| Fe | 195.45 | 34.35 | 31.70 | 141.04 | 54.15 |
| Ga | < 0.0002 | 0.05 | < 0.0002 | < 0.0002 | < 0.0002 |
| In | < 0.01 | < 0.01 | < 0.01 | < 0.01 | < 0.01 |
| K | 1260.81 | 2600.47 | 1164.71 | > 15000 | 3000.77 |
| Mg | 580.63 | 579.67 | 207.49 | 1000.73 | 652.85 |
| Mn | 39.44 | 6.52 | 3.07 | 23.03 | 11.57 |
| Mo | 1.62 | 0.02 | < 0.003 | 0.76 | 0.19 |
| Na | 217.37 | 112.50 | 5841.61 | 11177.19 | 54.78 |
| Ni | < 0.00004 | < 0.00004 | 0.38 | < 0.00004 | < 0.00004 |
| Pb | 1.64 | 0.33 | 0.05 | 1.00 | 0.31 |

| | | | | | |
|----|---------|---------|---------|---------|---------|
| Rb | 0.89 | 6.10 | 0.65 | 6.34 | 1.61 |
| Sr | 30.26 | 1.26 | 17.55 | 27.44 | 1.10 |
| Tl | < 0.001 | < 0.001 | < 0.001 | < 0.001 | < 0.001 |
| Zn | 38.11 | 11.12 | 4.74 | 17.69 | 10.44 |

Thermal characteristics

All thermal characteristics of the different thermogravimetric experiments at different heating rates can be found in Table S.2.

Table S.2 Characteristics of the thermogravimetric experiment at different heating rates:

| Biomass materials | B($^{\circ}\text{C min}^{-1}$) | $T_i(^{\circ}\text{C})$ | $T_{\max}(^{\circ}\text{C})$ | $T_f(^{\circ}\text{C})$ | $R_{\max}/(\text{min}^{-1})$ |
|------------------------|----------------------------------|-------------------------|------------------------------|-------------------------|------------------------------|
| Ciste de Monteplier CM | 2 | 200 | 334.88 | 361 | 0.25 |
| | 5 | 206 | 350.03 | 375 | 0.44 |
| | 10 | 210 | 359.95 | 395 | 0.98 |
| | 20 | 215 | 376.09 | 405 | 2.6 |
| | 30 | 224 | 383.69 | 430 | 2.3 |
| | 40 | 229 | 390.34 | 436 | 3.9 |
| Olive Kernels OK | 2 | 200 | 304.42 | 350 | 0.29 |
| | 5 | 209 | 318.18 | 375 | 0.51 |
| | 10 | 215 | 330.52 | 400 | 1.26 |
| | 20 | 221 | 343.81 | 425 | 2.88 |
| | 30 | 236 | 350.46 | 435 | 3.72 |
| | 40 | 240 | 356.16 | 441 | 4.46 |
| Aleppo Pine husks APH | 2 | 185 | 318.01 | 349 | 0.25 |
| | 5 | 198 | 333.37 | 375 | 0.64 |
| | 10 | 200 | 344.21 | 395 | 0.73 |
| | 20 | 205 | 358.06 | 405 | 2.83 |
| | 30 | 215 | 364.7 | 419 | 3.36 |
| | 40 | 219 | 371.35 | 440 | 4.75 |
| Straw wheat WS | 2 | 160 | 293.49 | 335 | 0.27 |
| | 5 | 165 | 310.58 | 365 | 0.71 |
| | 10 | 171 | 322.92 | 375 | 1.42 |
| | 20 | 370 | 334.32 | 365 | 2.44 |
| | 30 | 180 | 340.02 | 385 | 3.34 |
| | 40 | 185 | 345.71 | 395 | 5.45 |
| Date Kernels DK | 2 | 165 | 276.4 | 410 | 0.28 |
| | 5 | 171 | 285.9 | 447 | 0.48 |
| | 10 | 174 | 296.34 | 463 | 1.58 |
| | 20 | 190 | 306.78 | 474 | 3.41 |

| | | | | | |
|--|----|-----|--------|-----|------|
| | 30 | 198 | 313.43 | 489 | 4.47 |
| | 40 | 210 | 318.1 | 495 | 7.14 |

As discussed in the text, Figure S.1 and S.2 show the linearization of different samples according to KAS method and Coast Redferem.

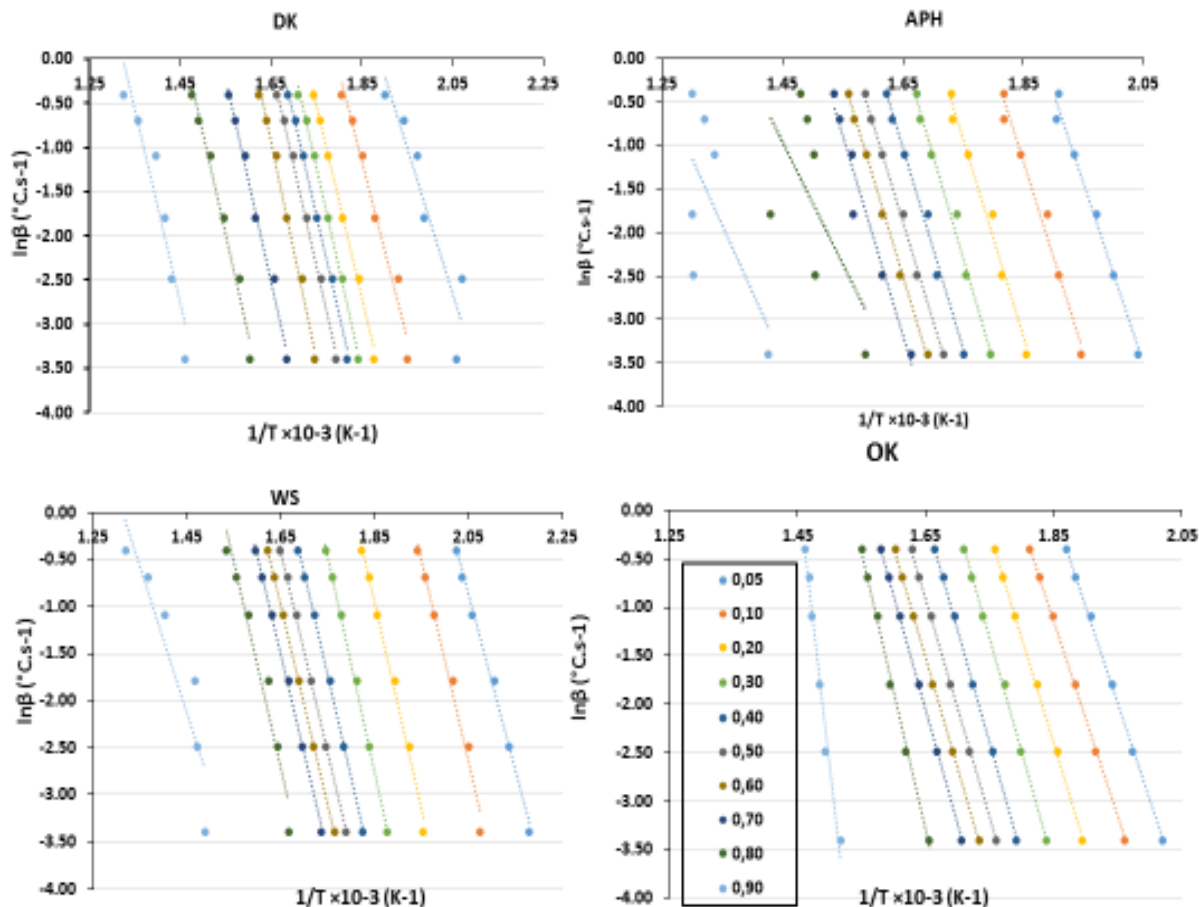


Figure S.1 KAS plots of OK, APH, WS and DK

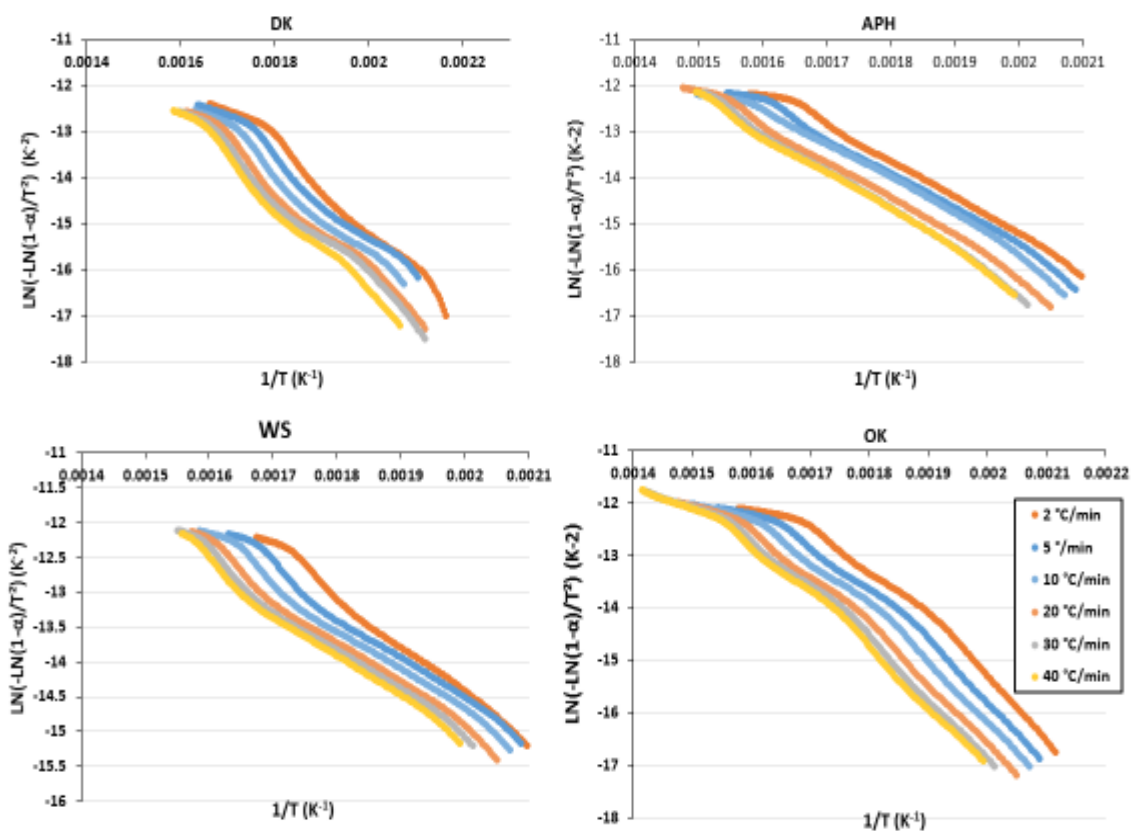


Figure S.2 Coast redferem plots of DK, APH, WS and OK

Kinetic parameters:

Table S.3 The activation energy and pre-exponential factor of CM, OK, APH, WS and DK according to KAS method.

| $\alpha/-$ | CM | | | OK | | | APH | | | WS | | | DK | | |
|------------|---------------------------|--------------------|-------|---------------------------|--------------------|-------|---------------------------|--------------------|-------|---------------------------|--------------------|-------|---------------------------|--------------------|-------|
| | $E_a(\text{kJ mol}^{-1})$ | $A(\text{s}^{-1})$ | R^2 |
| 0.05 | 193.03 | 1.31E+22 | 0.960 | 1.75E+02 | 2.39E+20 | 0.999 | 183.7 | 3.23E+21 | 0.987 | 164.2 | 4.17E+20 | 0.995 | 142.67 | 4.04E+17 | 0.876 |
| 0.1 | 187.28 | 8.19E+20 | 0.971 | 1.77E+02 | 1.21E+20 | 1.000 | 190.02 | 1.98E+21 | 0.978 | 187.64 | 1.98E+22 | 0.986 | 173.25 | 5.33E+19 | 0.973 |
| 0.15 | 183.93 | 1.67E+20 | 0.984 | 1.81E+02 | 1.59E+20 | 0.999 | 197.02 | 2.95E+21 | 0.981 | 191.9 | 1.15E+22 | 0.988 | 181.92 | 1.37E+20 | 0.989 |
| 0.2 | 189.38 | 2.61E+20 | 0.987 | 1.89E+02 | 5.01E+20 | 0.999 | 199.45 | 2.04E+21 | 0.985 | 194.19 | 6.16E+21 | 0.991 | 191.44 | 5.84E+20 | 0.995 |
| 0.25 | 190.88 | 1.85E+20 | 0.989 | 1.97E+02 | 1.35E+21 | 0.999 | 202.92 | 1.99E+21 | 0.986 | 200.11 | 8.45E+21 | 0.991 | 193.02 | 5.46E+20 | 0.997 |
| 0.3 | 194.31 | 1.93E+20 | 0.991 | 2.02E+02 | 2.48E+21 | 0.999 | 205.42 | 1.78E+21 | 0.987 | 201.16 | 4.64E+21 | 0.998 | 198 | 1.11E+21 | 0.996 |
| 0.35 | 196.31 | 1.57E+20 | 0.991 | 2.02E+02 | 1.37E+21 | 1.000 | 203.64 | 7.05E+20 | 0.984 | 196.76 | 9.08E+20 | 0.996 | 200.82 | 1.49E+21 | 0.996 |
| 0.4 | 196.98 | 9.82E+19 | 0.990 | 2.05E+02 | 1.45E+21 | 1.000 | 201.86 | 2.97E+20 | 0.988 | 190.21 | 1.33E+20 | 0.999 | 197.72 | 6.13E+20 | 0.996 |
| 0.45 | 200.95 | 1.24E+20 | 0.993 | 1.98E+02 | 2.29E+20 | 1.000 | 202.6 | 2.21E+20 | 0.995 | 191.22 | 1.05E+20 | 0.999 | 198.63 | 5.55E+20 | 0.997 |
| 0.5 | 199.68 | 6.01E+19 | 0.995 | 1.98E+02 | 1.66E+20 | 1.000 | 200.35 | 9.63E+19 | 0.997 | 187.85 | 3.67E+19 | 0.999 | 198.74 | 4.28E+20 | 0.995 |
| 0.55 | 197.2 | 2.46E+19 | 0.996 | 1.98E+02 | 1.08E+20 | 1.000 | 200.64 | 7.21E+19 | 0.998 | 185.63 | 1.75E+19 | 0.998 | 206.48 | 1.37E+21 | 0.995 |
| 0.6 | 198.81 | 1.61E+19 | 0.997 | 2.01E+02 | 1.17E+20 | 1.000 | 202.15 | 5.01E+19 | 0.997 | 187.46 | 1.37E+19 | 0.999 | 215.24 | 2.94E+21 | 0.991 |
| 0.65 | 195 | 5.78E+18 | 0.999 | 2.02E+02 | 9.97E+19 | 1.000 | 205.29 | 6.68E+19 | 0.993 | 186.4 | 8.59E+18 | 0.999 | 211.96 | 7.48E+20 | 0.989 |
| 0.7 | 194.59 | 4.02E+18 | 0.990 | 2.10E+02 | 3.60E+20 | 1.000 | 203.14 | 3.04E+19 | 0.951 | 187.65 | 8.34E+18 | 0.998 | 201.95 | 4.83E+19 | 0.991 |
| 0.75 | 193.99 | 1.89E+18 | 0.997 | 2.21E+02 | 1.26E+21 | 1.000 | 160.92 | 5.62E+15 | 0.681 | 200.09 | 4.29E+19 | 0.991 | 191.54 | 2.21E+18 | 0.996 |
| 0.8 | 187.2 | 4.92E+17 | 0.988 | 2.56E+02 | 6.31E+23 | 0.997 | 122.82 | 3.23E+12 | 0.383 | 190.31 | 4.24E+18 | 0.955 | 198.89 | 4.77E+18 | 0.982 |
| 0.85 | 177.14 | 2.26E+16 | 0.933 | 3.41E+02 | 7.59E+29 | 0.997 | 135.97 | 1.05E+13 | 0.427 | 163.8 | 7.26E+15 | 0.886 | 211.91 | 1.09E+19 | 0.967 |
| 0.9 | 154.34 | 8.49E+13 | 0.919 | 4.95E+02 | 1.39E+40 | 0.976 | 135.14 | 2.21E+12 | 0.428 | 137.33 | 1.23E+13 | 0.846 | 193.91 | 9.52E+16 | 0.908 |
| 0.95 | 134.05 | 4.47E+11 | 0.869 | 7.14E+02 | 1.34E+53 | 0.981 | 120.7 | 3.85E+10 | 0.465 | 101.22 | 5.57E+9 | 0.823 | 121.98 | 1.20E+11 | 0.811 |

Activation energy and pre-exponential factor according to Coats and Redfern method are shown in Table S.4. The variation in the value of E_a with the different heating rates can be explained by the experimental error, on one hand, and by the limitations of heat transfer, which tended to increase with high heating rates, on the other hand. The error on E_a and A according to Coats Redfern method reported in Table S.5 has been calculated with respect to the different heating rates.

Table S.4: Detailed kinetic parameters according to Coats–Redfern method.

| | $\beta(\text{°C min}^{-1})$ | $E_a(\text{kJ mol}^{-1})$ | $A(\text{s}^{-1})$ | R^2 |
|-----|-----------------------------|---------------------------|--------------------|-------|
| CM | 2 | 73.92 | 1.94E+03 | 0.979 |
| | 5 | 70.95 | 4.26E+03 | 0.982 |
| | 10 | 73.21 | 8.10E+03 | 0.979 |
| | 20 | 76.64 | 1.57E+04 | 0.988 |
| | 30 | 69.95 | 1.98E+04 | 0.988 |
| OK | 40 | 75.67 | 2.64E+04 | 0.990 |
| | 2 | 75.87 | 2.71E+03 | 0.971 |
| | 5 | 73.33 | 5.71E+03 | 0.977 |
| | 10 | 71.83 | 9.76E+03 | 0.977 |
| | 20 | 76.15 | 1.81E+04 | 0.983 |
| WS | 30 | 73.04 | 2.27E+04 | 0.978 |
| | 40 | 74.27 | 2.69E+04 | 0.981 |
| | 2 | 59.87 | 5.61E+01 | 0.981 |
| | 5 | 53.82 | 1.17E+02 | 0.987 |
| | 10 | 53.34 | 2.15E+02 | 0.986 |
| APH | 20 | 54.01 | 4.04E+02 | 0.989 |
| | 30 | 53.94 | 5.62E+02 | 0.986 |
| | 40 | 53.86 | 6.96E+02 | 0.988 |
| | 2 | 67.42 | 5.02E+02 | 0.996 |
| | 5 | 64.19 | 1.11E+03 | 0.996 |
| DK | 10 | 60.67 | 1.97E+03 | 0.988 |
| | 20 | 67.52 | 4.10E+03 | 0.996 |
| | 30 | 68.12 | 5.82E+03 | 0.995 |
| | 40 | 66.84 | 7.15E+03 | 0.996 |
| | 2 | 76.04 | 7.73E+02 | 0.926 |
| | 5 | 72.03 | 1.70E+03 | 0.941 |
| | 10 | 75.84 | 3.33E+03 | 0.951 |
| | 20 | 77.39 | 6.31E+03 | 0.969 |
| | 30 | 77.26 | 8.77E+03 | 0.976 |
| | 40 | 82.08 | 1.15E+04 | 0.974 |